

This is a repository copy of *The role of interfacial intermixing on HAMR dynamics in bilayer media*.

White Rose Research Online URL for this paper:

<https://eprints.whiterose.ac.uk/192960/>

Version: Accepted Version

Article:

Meo, A., Chureemart, P., Chantrell, R. W. orcid.org/0000-0001-5410-5615 et al. (1 more author) (2022) The role of interfacial intermixing on HAMR dynamics in bilayer media. *Journal of physics. Condensed matter : an Institute of Physics journal*. 465801. ISSN 1361-648X

<https://doi.org/10.1088/1361-648X/ac916d>

Reuse

This article is distributed under the terms of the Creative Commons Attribution-NonCommercial-NoDerivs (CC BY-NC-ND) licence. This licence only allows you to download this work and share it with others as long as you credit the authors, but you can't change the article in any way or use it commercially. More information and the full terms of the licence here: <https://creativecommons.org/licenses/>

Takedown

If you consider content in White Rose Research Online to be in breach of UK law, please notify us by emailing eprints@whiterose.ac.uk including the URL of the record and the reason for the withdrawal request.

The role of interfacial intermixing on HAMR dynamics in bilayer media

A. Meo*

Department of Physics, Maharakham University, Maharakham 44150, Thailand

P. Chureemart

Department of Physics, Maharakham University, Maharakham 44150, Thailand

R. W. Chantrell[†]

Department of Physics, University of York, York YO10 5DD, United Kingdom

J. Chureemart[‡]

Department of Physics, Maharakham University, Maharakham 44150, Thailand

We use an atomistic spin model to simulate FePt-based bilayers for heat assisted magnetic recording (HAMR) devices and investigate the effect of various degrees intermixing that might arise throughout the fabrication, growth and annealing processes, as well as different interlayer exchange couplings, on HAMR magnetisation dynamics. Intermixing can impact the device functionality, but interestingly does not deteriorate the properties of the system. Our results suggest that modest intermixing can prove beneficial and yield an improvement in the magnetisation dynamics for HAMR processes, also relaxing the requirement for weak exchange coupling between the layers. Therefore, we propose that a certain intermixing across the interface could be engineered in the fabrication process to improve HAMR technology further.

I. INTRODUCTION

Heat assisted magnetic recording (HAMR) technology is now considered the future candidate for high density storage applications [1–8]. HAMR exploits the effect of local heating on the magnetic layer during the writing process to reduce the coercive field of the high anisotropy grains, therefore making possible to reverse the magnetisation and write the information. To achieve areal density as large as 4 Tb/in² optimisation of both the medium properties and writing/reading mechanisms is required. A path to improve HAMR performances is to engineer the magnetic layer by coupling the hard iron-platinum (FePt) grains, characterised by large magnetic anisotropy, with grains that are soft and have higher Curie temperature (T_c) than FePt [9–18]. At temperatures close to T_c^{FePt} where FePt loses its ferromagnetic character, the softer material remains ferromagnetic with a non-zero magnetisation and a weak anisotropy. Consequently the external field acts on the soft phase only and, due to the low anisotropy a lower magnitude than for a single phase medium is required. As the system cools down the hard material anisotropy is restored, resulting in parallel alignment of the magnetisation of the hard and soft phases. Such a coupled structure, with optimised interlayer exchange coupling, allows magnetisation switching at reduced write fields and temperatures.

Sputtering is the most commonly employed fabrication technique on an industrial scale. However it is difficult to achieve atomically smooth interfaces, and some interface mixing resulting from atomic migration across an interface might be expected. This has not been considered widely for HAMR

technology, neither experimentally [19] nor theoretically, due to the complex nature of the phenomenon. The realm of this process falls naturally within the atomistic description as it involves changes of the atomic composition at the interface. For these reasons in this work we focus on the effect of intermixing between the two different magnetic layers on the system properties and magnetisation dynamics, and we perform the investigation by means of an atomistic spin model. Our simulations allow to propose that the deposition and fabrication processes could be engineered to achieve an optimal intermixing degree resulting in “locally graded media” leading to improved media functionality.

II. METHODS

For the simulation of spin dynamics and HAMR processes we employ an atomistic spin model as implemented in the freely distributed software package VAMPIRE [20]. The dynamics of each individual atomic spin is modelled by integrating the Landau-Lifshitz-Gilbert (LLG) equation of motion [21]:

$$\frac{\partial \mathbf{S}_i}{\partial t} = -\frac{\gamma_e}{1+\lambda^2} [\mathbf{S}_i \times \mathbf{H}_{\text{eff}}^i + \lambda \mathbf{S}_i \times (\mathbf{S}_i \times \mathbf{H}_{\text{eff}}^i)], \quad (1)$$

where \mathbf{S}_i is the unit vector of the atomic spin on site i , γ_e is the absolute value of the electron gyromagnetic ratio, λ is the Gilbert damping that couples the spin system to the heat bath. $\mathbf{H}_{\text{eff}}^i$ is the effective field acting on spin i and accounts for the interactions within the spin system (exchange, anisotropy and Zeeman coupling) and thermal effects via a stochastic term represented by a Langevin thermostat [21].

We describe the system as a bilayer where there exists a direct interface between the two layers and these are magnetically coupled via direct exchange. One layer is FePt and

* andrea.m@msu.ac.th

[†] roy.chantrell@york.ac.uk

[‡] jessada.c@msu.ac.th

the other is a iron-based (Fe-based) alloy (Soft). In realistic HAMR media it is likely to expect the presence of an exchange break layer (EBL), i.e. an atomic thin layer either non magnetic or weakly magnetic, separating the two layers. Nevertheless, being this the first investigation, we rely on the aforementioned simplification. Moreover, previous experimental studies on FePt-based multilayer systems with no EBL for perpendicular recording media (PMR) applications have shown that by tweaking the growth temperature and annealing condition the magnetic properties, such as coupling at the interface and anisotropy, can be altered [22–27]. We model the system as an hexagonal grain with in-plane dimension 5 nm and variable thickness between 10 and 15 nm, where the top 5 nm are composed of Fe-based alloy and the rest is FePt. *Ab initio* calculations by Mryasov *et al* [28] have found that in L_{10} -ordered FePt the Pt moment has a delocalised nature and is induced by Fe. By exploiting this dependence, they proposed a description of FePt that considers Fe only and accounts for Pt effects via an enhanced effective moment (Fe+Pt), and a long range exchange coupling that includes two-ion anisotropy [28, 29]. For the sake of computational efficiency, we simplify the long range Hamiltonian by modelling FePt with an isotropic nearest-neighbour Hamiltonian with uniaxial anisotropy, similarly to the works of Ababei *et al* [18, 30] and Strungaru *et al* [31], by mapping the original tetragonally distorted face-centre-cubic structure of FePt to a distorted simple cubic lattice of dimensions $a_{0,xy} = 0.272$ nm and $a_{0,z} = 0.385$ nm. Within this approach we assign FePt a uniaxial anisotropy energy of $k_u^{\text{FePt}} = 2.63 \cdot 10^{-22}$ J atom $^{-1}$, an atomic magnetic moment $\mu_s^{\text{FePt}} = 3.23 \mu_B$ and an exchange coupling $J_{ij}^{\text{FePt}} = 6.8 \cdot 10^{-21}$ J link $^{-1}$. These give $T_c \sim 700$ K, $K_u \sim 9 \cdot 10^6$ Jm $^{-3}$ and $M_s \sim 1 \cdot 10^6$ Jm $^{-3}$ T $^{-1}$ as in bulk FePt [5, 32–34]. The Fe-based alloy is characterised by $J_{ij} = 9.5 \cdot 10^{-21}$ J link $^{-1}$, $k_u = 1 \cdot 10^{-23}$ J atom $^{-1}$ and $\mu_s = 2.15 \mu_B$. These parameters are derived from experimental bulk values of a magnet with relatively low anisotropy and high T_c : $M_s = 7 \cdot 10^5$ JT $^{-1}$ m $^{-3}$, $T_c \sim 1,000$ K and anisotropy field $H_{\text{ani}} = 1$ T. We assume $\lambda = 0.1$ for FePt as done in our previous work [35], a value accepted normally for compounds including heavy elements such as Pt and in agreement with the value reported in literature [18, 36]. We also assign the same damping to the soft layer, given that this can prove beneficial for HAMR [18]. The simulated temperature dependent magnetisation of individual $5 \times 5 \times 5$ nm 3 FePt and soft phase grains is presented in Fig. 1. The figure allows to appreciate the different T_c of the two materials as well as finite size effect, which result in a non-critical behaviour of the magnetisation for temperatures approaching T_c with $T_c^{\text{FePt}} \sim 700$ K, and a non-zero tail above it. We stress that to obtain the two curves the two materials are simulated as individual systems, thus there is no coupling between them here. We vary the exchange coupling between FePt and soft phase (J_{int}) between 10 and 30% of J_{ij}^{FePt} to mimic the presence of an EBL; the lower bound ensures that the system is coupled, whilst the upper bound guarantees we are within the exchange spring limit. These parameters are listed in Table I.

The degree of intermixing is varied from 0%, i.e. an ideally smooth interface, up to 15%. Larger values are not considered

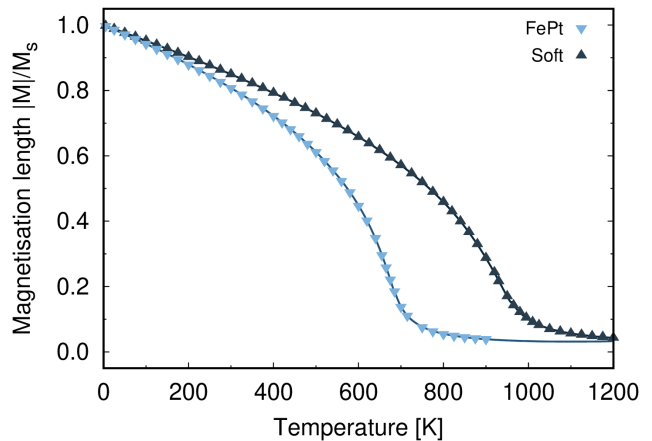


FIG. 1. Calculated temperature-dependent magnetisation length ($m = |\mathbf{M}|/M_s(0\text{K})$) for $5 \times 5 \times 5$ nm 3 FePt (light-blue downwards triangles) and soft phase (dark-blue upward triangles) grains performing LLG simulations with a time-step of $1 \cdot 10^{-16}$ s. Continuous lines are fit to the data according to Eq. 14 of Ref. [35], which gives Curie temperatures of 690 K for FePt and 990 K for the soft material. Finite size effects can be clearly seen in the non-zero tail of m after the critical temperature. The spin system is integrated for 100,000 steps of which the initial 50,000 steps are for reaching thermal equilibrium; the LLG equation is integrated with a time-step $dt = 1 \cdot 10^{-16}$ s.

TABLE I. Simulation parameters for the bilayer systems.

| | FePt | Soft | Unit |
|----------------------------------|-----------------------|----------------------|----------------|
| Exchange energy J_{ij} | $6.8 \cdot 10^{-21}$ | $9.5 \cdot 10^{-21}$ | J link $^{-1}$ |
| Uniaxial anisotropy energy k_u | $2.63 \cdot 10^{-22}$ | $1.0 \cdot 10^{-23}$ | J atom $^{-1}$ |
| Atomic magnetic moment μ_s | 3.63 | 2.15 | μ_B |
| Gilbert damping λ | 0.10 | 0.10 | |

as they yield an alloyed FePt-soft system in the soft region, thus diverging from the aim of this work. The intermixing is simulated by randomly replacing atoms within one material with atoms of the other with a certain probability; a sketch of the systems is presented in Figure 2. We emphasise that alternative models that allow to treat the Pt explicitly are required to properly describe effects such as intermixing, where the Fe and Pt atoms can behave differently depending on the site location. In such a case in fact, the description of FePt where the Pt contribution is included via an effective augmented atomic spin moment starts losing its validity. There are reports of models that, by taking into consideration longitudinal spin fluctuations, can include Pt explicitly and allow for Pt magnetic moments to vary with the surrounding Fe environment [37]. Such an approach requires a detailed parameterisation of both Fe and Pt magnetic properties and efforts are on the way to develop an approach similar to that proposed by Ellis *et al*. Moreover, the approximation of a weak exchange coupling between effective FePt atoms and those of the soft material when these are displaced in the opposite layer can be seen as a representation of the exchange coupling on

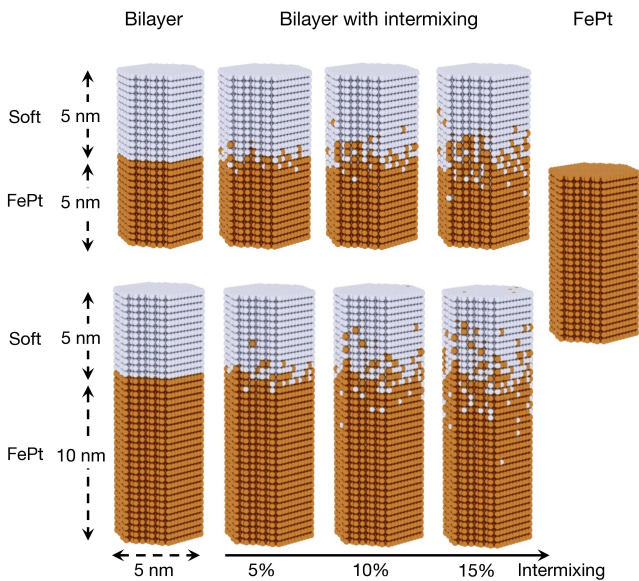


FIG. 2. Sketch of the investigated systems: on the left a Soft/FePt hexagonal grain of dimensions $5 \times 5 \times 15 \text{ nm}^3$ without intermixing; in the centre the same system with increasing degree of intermixing from small to large; on the right a $5 \times 5 \times 10 \text{ nm}^3$ FePt hexagonal grain. Each sphere represents an atomic magnetic moment: silver for the soft phase (Soft) and gold for FePt.

average between Fe-soft material atoms and Pt-soft-material atoms. Taking this into consideration and given the lack of a better model to describe the intermixing, our work represents an initial effort to simulate and investigate this phenomenon and the possible implications.

We adopt a simplified description of a HAMR process where the external field and heat pulse are applied to the region underneath the writing head. We model the laser pulse ($T(t)$) as a spatially uniform temperature pulse with Gaussian time profile:

$$T(t) = T_a + (T_{\text{peak}} - T_a) \exp \left[- \left(\frac{t - 3t_{\text{pulse}}}{t_{\text{pulse}}} \right)^2 \right], \quad (2)$$

where T_a is the temperature at which the system is left when no pulse is applied, ambient temperature, and T_{peak} is the maximum temperature, reached at $3t_{\text{pulse}}$, where t_{pulse} is one sixth of the total duration of the pulse. HAMR dynamics is obtained by simulating individual grains and repeating each simulation 100 times with a different random seed to ensure a large enough statistical ensemble. Given the fast nature of the process and the high temperatures involved, we adopt an integration step of $1 \cdot 10^{-16} \text{ s}$ in our atomistic simulations. The switching probability is then given by the number of successful switching events over the 100 total repetitions. Following Ref.[35], a cumulative distribution function can be used to fit the switching probability as a function of peak temperature.

III. RESULTS

To understand the effect of the interfacial coupling on the switching properties during HAMR processes, we consider values of J_{int} corresponding to 10, 15 and 30% of J_{ij}^{FePt} . However for the sake of clarity when presenting the results, only data for 10 and 30% is shown. We simulate temperature pulses by varying pulse time t_{pulse} from 100 to 300 ps and peak temperature T_{peak} from 550 to 750 K, under an external magnetic field H_{app} of 1 T. We compare the results for the bilayer systems with those for pure FePt for the same HAMR setup. The latter have already been published by the authors elsewhere [35] and serve as a benchmark comparison.

A. Ideal interface

Figure 3 presents the switching probabilities for bilayers with ideal interfaces of thickness 10 nm (a,b) and 15 nm (c,d) for $J_{\text{int}} = 10$ and 30% of J_{ij}^{FePt} ($0.68 \cdot 10^{-21}$, $2.04 \cdot 10^{-21} \text{ Jlink}^{-1}$). For a single material the magnetisation reversal occurs within the recording window where the external field is larger than the grain anisotropy field reduced by the temperature pulse [5]. In the case of an exchange coupled system where the recording layer has a lower anisotropy and a higher T_c , the recording window can be enlarged. This makes possible to achieve the reversal at lower T_{peak} . However, the width of the recording window depends on the strength of the coupling and pulse duration. Below 650 K the magnetisation reversal in FePt is expected to follow a precessional dynamics, which depends on the anisotropy field mainly, whilst it becomes close to linear at higher temperatures [35]. FePt grains do not reverse at these temperatures, but the composite system could yield switching via proper engineering of the material properties. The aim is to reduce the peak temperature required for the reversal without impacting negatively either on the distribution width or the maximum value of the switching probability. By inspection of Figure 3(a,b) we find that the bilayer switching probability shifts towards lower T_{peak} . However, this is also accompanied by a widening of the same. This can prove detrimental for transition width and the bit error rate properties. Since precessional switching is a slower process than linear dynamics, as t_{pulse} increases from 100 to 300 ps more and more grains reverse their magnetisation and, therefore, we can expect a shift of the switching probability towards lower temperatures. In fact, this is observed in both the investigated systems, both FePt and bilayers. It is worth mentioning that the processes investigated here correspond to a fast dynamics if compared with a continuous HAMR process, analogous to a head speed around 20 m/s. This is a major factor in determining the switching properties and should be taken into account in the analysis. We note that for the bilayer system 10 nm tall, the switching probability curves for very short temperature pulses reach lower maximum values and exhibit wider transition width for stronger J_{int} . This represents a net difference with respect to pure FePt grains, where the maximum seems to depend on the applied field solely. The lower maximum switching probability for short pulses and el-

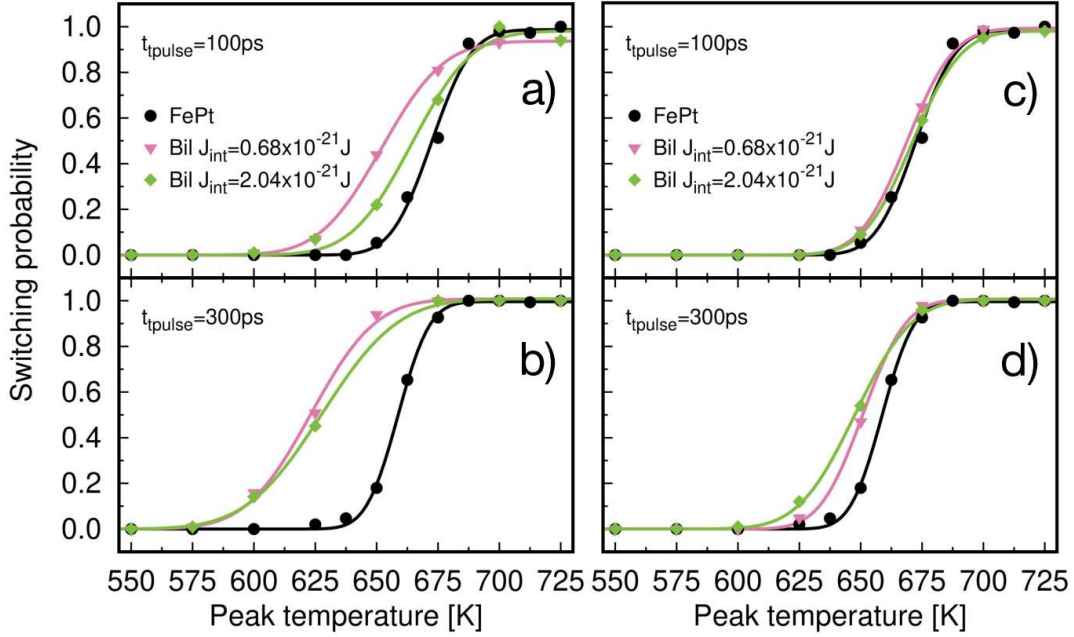


FIG. 3. Comparison of the switching probability as a function of peak temperature T_{peak} for a pulse length t_{pulse} of 100 ps (a,c) and 300 ps (b,d) among FePt (black dots) and ideal bilayer grains with J_{int} 10% (downward triangles) and 30% (diamonds) of J_{ij}^{FePt} for grain thickness 10 nm in a) and b), and 15 nm in c) and d). Full symbols represent the data and lines are fit to a cumulative function.

evated T_{peak} is likely caused by the fast cooling rate that does not allow the FePt layer to follow the reversal of the soft layer. Once the FePt recovers the high anisotropy, if its magnetisation has not reversed, it drives the reversal of the soft layer back to the initial state, and the switching results unsuccessful. This does not occur for the thicker grain since the grains at large temperatures are dominated by the FePt behaviour. This emphasises how tuning the pulse properties is crucial to achieve a successful and efficient switching.

If we fix t_{pulse} , we observe that the width of the switching probability increases with J_{int} . As the coupling increases the system tends towards the rigid magnet behaviour: for T_{peak} below the linear regime of FePt the total coercivity of the bilayer decreases with a progressive loss of the exchange spring effect. This results in a larger probability of reversing the grain magnetisation at low T_{peak} . When T_{peak} falls in the range of temperatures of FePt linear dynamics, FePt dominates the reversal process. This occurs for both the investigated thickness, with the bilayer and pure FePt grains switching probabilities are nearly the same for T_{peak} above 675 K. Longer pulses result in a wider recording window, and thus a slightly larger switching probability across these temperatures. Overall, a stronger J_{int} comports a broader switching probability distribution, hence a larger transition width, than obtained in pure FePt grains. This is not ideal for applications, where a narrow switching distribution is desirable.

Our results show that a bilayer system composed half of FePt and half of a soft material is not a suitable choice to replace media of pure FePt due to the widening of the switching probability and the reaching a lower maximum value of the same. On the other hand, our simulations suggest that

when FePt makes most of the grain, if J_{int} does not exceed 10% of J_{ij}^{FePt} , it becomes possible to successfully exploit the exchange spring mechanism reducing the maximum temperature required for the reversal up to 15 K for the slowest process. Other ways to improve the performances of coupled bilayer system could be to choose a couple of materials with a different damping, as discussed in Ref. [18].

B. Interface with intermixing

Once the properties of grains with an ideal interface have been characterised, we investigate the effect of interfacial intermixing by varying the degree of intermixing as a function of the exchange coupling between hard and soft phase. The structures with intermixing are sketched in the central region of Figure 2. One would expect that the main effect of intermixing is to induce a broader dispersion of the switching probability due to a smearing of the magnetic properties. In Figure 4 we compare the switching probabilities of the bilayer with intermixing (diamonds, squares and upward triangles) with those of FePt grains (dots) and bilayer without intermixing (downwards triangles) for $t_{\text{pulse}} = 300$ ps for different J_{int} for bilayer thickness of 10 nm and 15 nm in panels (a,b) and (c,d) respectively. Surprisingly, we find that the intermixing does not cause the switching probability to deteriorate, and in most of the investigated cases the switching probabilities show both a shift towards lower peak temperatures and a reduced width of the distribution. In fact, by inspection of the figures it emerges clearly how the switching probability reaches the maximum at a lower T_{peak} as the intermixing increases.

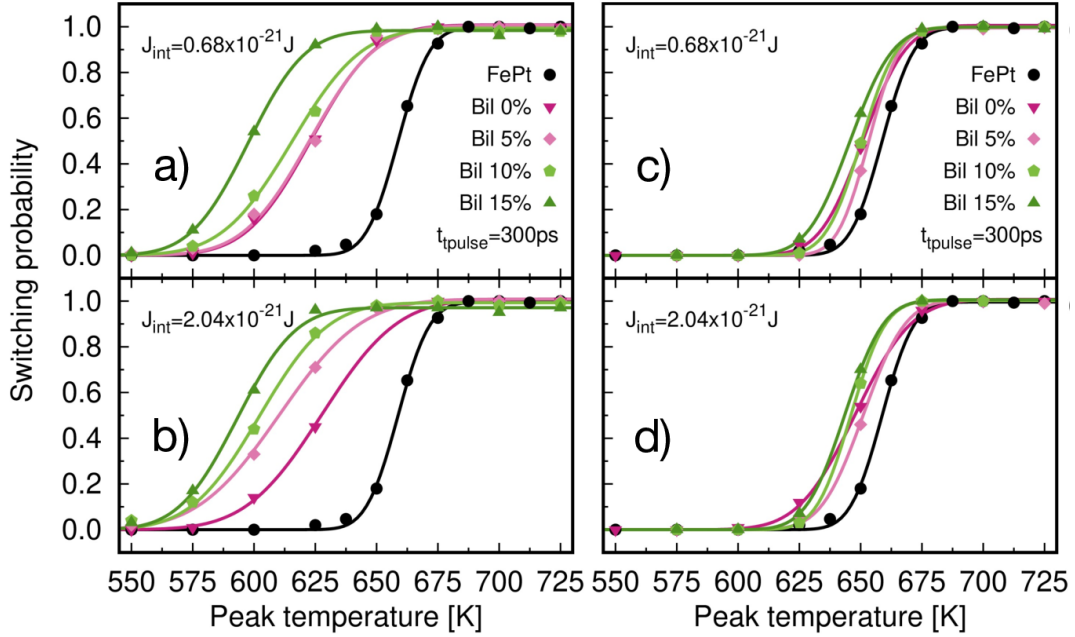


FIG. 4. Plot of the switching probability for a $5 \times 5 \times 15 \text{ nm}^3$ hexagonal bilayer grain comparing J_{int} 10% (a,c) and 30% (b,d) of J_{ij}^{FePt} as a function intermixing and peak temperature T_{peak} for a pulse length $t_{\text{pulse}} = 300 \text{ ps}$. a) and b) are for bilayers with thickness 10 nm, c) and d) for thickness 15 nm. These switching probabilities are compared with those of FePt (black dots). Full symbols represent the data and lines are fit to a cumulative function.

Counter intuitively, interfacial intermixing yields larger improvements in the grains with thickness 10 nm, with a shift of 25 K with respect to the bilayer with ideal interface and more than 50 K with respect to pure Fe grains. We can expect that intermixing in the system composed of half FePt and half soft material results in an average properties system with a softer nature with respect to the thicker system, therefore resulting in switching at lower temperatures. Interestingly, we also find that the difference between different J_{int} tends to decrease for the strongest exchange coupling values. Not only, but the strongest J_{int} yield a shift towards lower temperatures and narrow distribution of the switching probability. This occurs for both the thicknesses, as it can be seen by comparing panels b) and d) of Figure 4. As demonstrated by our results for the bilayer with ideal interface, minimising the coupling at the interface is usually favourable. The fact that the strength of the coupling has a weaker impact on the switching properties of the grains and that diluting the coupling might not be necessary, could prove beneficial in the material processing and development of HAMR devices.

In order to understand the origin of these changes, we consider an average system where to each spin within an atomic layer is assigned the average of the layer magnetic properties. This is done for the different degrees of intermixing, and the average is performed over 100 grains each generated with a different random seed to ensure a different structure. As an example we plot the average zero temperature layer exchange coupling J_{ij} and anisotropy field ($H_{\text{ani}} = 2k_u/\mu_s$) for $J_{\text{int}} = 10\%$ of J_{ij}^{FePt} for the 15 nm thick grains, presented in Figure 5. Intermixing affects the grains by causing a gradient

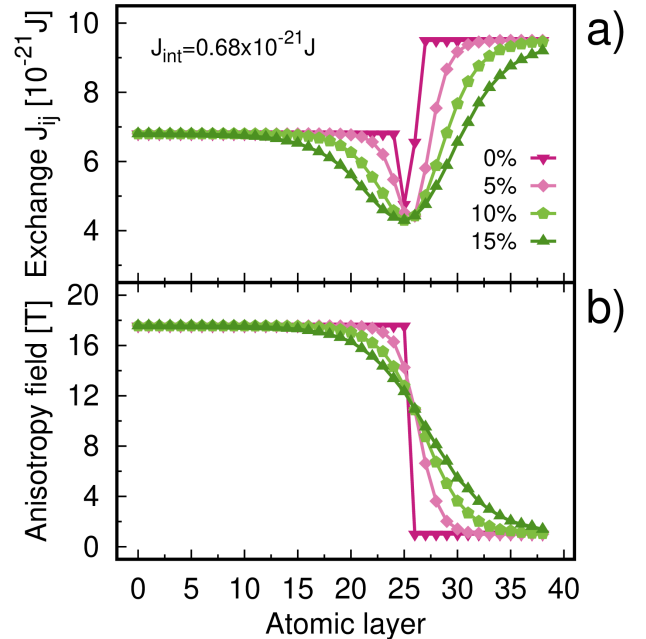


FIG. 5. Averaged layer resolved zero temperature exchange coupling (a) and anisotropy field (b) for $J_{\text{int}} = 10\%$ of J_{ij}^{FePt} ($0.68 \cdot 10^{-21} \text{ Jlink}^{-1}$) comparing different intermixing.

of the magnetic properties across the thickness of the grain. Let us consider the exchange coupling in panel a): in the ideal interface case only the interfacial layers are characterised by

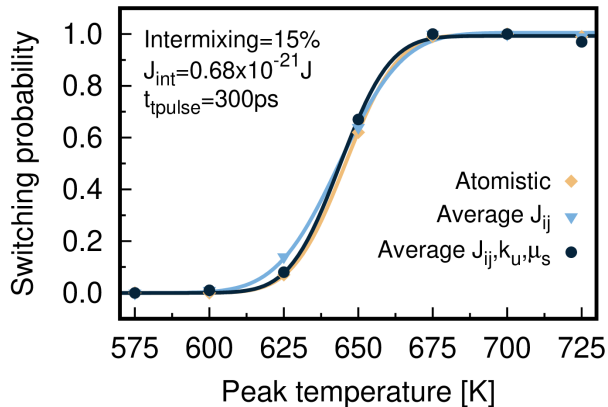


FIG. 6. Comparison of the switching probability as a function of peak temperature T_{peak} for a pulse length $t_{\text{pulse}} = 300\text{ps}$ of a bilayer grain characterised by 15% intermixing and $J_{\text{int}} = 10\%$ of J_{ij}^{FePt} ($0.68 \cdot 10^{-21} \text{Jlink}^{-1}$) with those of an equivalent system where each layer is characterised by the averaged properties. Full symbols represent the data and lines are fit to a cumulative function.

a lower exchange, shown by the violet line and downwards triangles. As the intermixing increases, a larger number of layers near the interface is characterised by a lower J_{ij} . This yields an average lower coupling in the whole grain, and in particular in the soft phase region. These layers are more loosely coupled than in the ideal interface case and, thus, are less thermally stable. This drop could also explain the progressive attenuation in the difference between small and large J_{int} observed above. In fact, the spins at the interface would behave as they were characterised by a lower J_{int} effectively. Moreover, since T_c is mainly determined by the exchange coupling [38], grains with intermixing across the interface will be characterised by a lower T_c . In turn, because T_c affects the temperature dependence of macroscopic magnetisation and anisotropy, we can expect a weaker anisotropy field H_{ani} at elevated temperature. The intermixing is also responsible for an independent gradient of H_{ani} , shown in panel b), due to the layer averaging of k_u and μ_s : H_{ani} decreases close to the interface in FePt and increases in the other layer. This is similar to graded-anisotropy systems, for instance obtained by argon-ion (Ar+) irradiation of FePt films studied by di Bona *et al* [39] for PMR applications. In light of this analysis, we can understand the better switching performances for thickness 10 nm. While in the thicker system the drop in the exchange does not affect the bottom of the grain where the atomic properties remain those of FePt, nearly the whole grain is affected for the thinner case. As a consequence, on average the grain is characterised by a weaker exchange coupling. Similarly, H_{ani} varies smoothly across the whole grain in the thin case.

To determine which of these effects, exchange and anisotropy variation, is dominant or whether they are in competition, we simulate a HAMR process for a system of thickness 15 nm with 15% of intermixing and $J_{\text{int}} = 10\%$ of J_{ij}^{FePt} in two cases: one where the exchange coupling J_{ij} , anisotropy

k_u and magnetic moment μ_s are replaced by their atomic layer average values; the other where only the exchange is replaced with the atomic layer average value, while k_u and μ_s are those of the ideal interface grain. We compare the obtained switching probabilities as a function of T_{peak} in Figure 6. Both approximations yield a switching probability close to that of the original atomic system and are centred at the same T_{peak} . This confirms that the reduction of the exchange is indeed the major factor in the improvement of the switching properties. When J_{ij} , k_u and μ_s are replaced by their layer-average value the switching probability matches that of the atomistic system. Instead, if only J_{ij} is averaged, the switching probability has a broader distribution. This can be explained by considering that a larger H_{ani} of the soft phase ($H_{\text{ani}}^{\text{soft}}$) reduces the probability that a grain is reversed at low T_{peak} , and a lower H_{ani} of FePt ($H_{\text{ani}}^{\text{FePt}}$) increases the probability at high T_{peak} . We note that the effect at low T_{peak} , where we expect the soft material to be dominant, is consistent with the results in graded exchange coupled composite media for PMR where a decreasing anisotropy as a function of thickness yields a reduction of the switching field [9, 10].

Finally, to further confirm the importance and the role of the local variation of J_{ij} across the interface, we compare the intermixed system with other two similar systems. One, discussed in Supplementary note 1, is a simple model of bilayer with EBL. We find that when the EBL extends over 3 or 4 monolayers the system with EBL exhibits an analogous behaviour to the intermixing case due to an effective decrease in the exchange coupling across the interface. The other, presented in Supplementary note 2, is a “linearly varying Curie temperature medium”: a system whose J_{ij} is varied linearly from J_{ij}^{FePt} to J_{ij}^{Soft} , similarly to Ref.[40]. The linear gradient of T_c yields switching at temperatures larger than T_c^{FePt} and thus it proves the critical role of a local decrease in J_{ij} rather than a linear or non-monotonic variation in J_{ij} (T_c). The fact that the variation in the interlayer exchange coupling, rather than the magnetic moments and anisotropy energies, is the key player in the changes and improvements in the switching properties validates the proposed approach to describe the intermixing phenomenon. As such, we expect the main features of our results to be confirmed by more refined models once these will be accessible.

IV. CONCLUSIONS

In conclusion, we have investigated the effect of different interlayer exchange coupling and made an initial effort to study the effect of intermixing on HAMR magnetisation dynamics of FePt/Soft-phase bilayer grains by means of atomistic spin simulations. Replacing pure FePt grains with exchange coupled composites systems made of FePt and a soft Fe-like material would allow to reduce the maximum temperature required to switch the grain magnetisation. Our results suggest that it is possible to improve the performance of HAMR systems by engineering the interlayer coupling to be around 10% of J_{ij}^{FePt} when FePt makes most of the grain. Instead, the switching at lower temperatures is counteracted by

a widening in the switching probability when half of the grain is FePt. Interestingly we find that intermixing does not degrade the switching properties of the bilayer system. It yields better switching performances than single FePt grains. Intermixing is responsible for a region across the interface with low exchange coupling and this results in a net improvement in the switching probability even for a system with large interlayer coupling for a modest interfacial intermixing. Moreover, an even grain composition results in improved switching performances yielding switching at lower temperatures. This could prove beneficial due to the reduced demand of material and overall thickness of the magnetic film. On the basis of these results we propose that deposition, growth and fabrication processes could be engineered to achieve an optimal in-

termixing degree resulting in “locally graded media” leading to improved media functionality.

ACKNOWLEDGMENTS

JC would like to acknowledge the financial support from Mahasarakham University. The authors gratefully acknowledge the funding from Transforming Systems through Partnership Programme of the Royal Academy of Engineering under Grant No. TSP1285 and Seagate Technology (Thailand). The simulations were undertaken on the VIKING cluster, which is a high-performance compute facility provided by the University of York.

-
- [1] D. Weller, G. Parker, O. Mosendz, E. Champion, B. Stipe, X. Wang, T. Klemmer, G. Ju, and A. Ajan, A HAMR media technology roadmap to an areal density of 4 Tb/in², IEEE Transactions on Magnetics **50**, 1 (2014).
- [2] M. Kryder, E. Gage, T. McDaniel, W. Challener, R. Rottmayer, Ganping Ju, Yiao-Tee Hsia, and M. Erden, Heat assisted magnetic recording, Proceedings of the IEEE **96**, 1810 (2008).
- [3] R. E. Rottmayer, S. Batra, D. Buechel, W. A. Challener, J. Hohlfield, Y. Kubota, L. Li, B. Lu, C. Mihalcea, K. Mountfield, K. Pelhos, C. Peng, T. Rausch, M. A. Seigler, D. Weller, and X. M. Yang, Heat-Assisted magnetic recording, IEEE Transactions on Magnetics **42**, 2417 (2006).
- [4] G. Ju, Y. Peng, E. K. Chang, Y. Ding, A. Q. Wu, X. Zhu, Y. Kubota, T. J. Klemmer, H. Amini, L. Gao, Z. Fan, T. Rausch, P. Subedi, M. Ma, S. Kalarickal, C. J. Rea, D. V. Dimitrov, P. W. Huang, K. Wang, X. Chen, C. Peng, W. Chen, J. W. Dykes, M. A. Seigler, E. C. Gage, R. Chantrell, and J. U. Thiele, High Density Heat-Assisted Magnetic Recording Media and Advanced Characterization - Progress and Challenges, IEEE Transactions on Magnetics **51**, 1 (2015).
- [5] D. Weller, G. Parker, O. Mosendz, A. Lyberatos, D. Mitin, N. Y. Safonova, and M. Albrecht, Review Article: FePt heat assisted magnetic recording media, Journal of Vacuum Science & Technology B **34**, 060801 (2016).
- [6] C. Rea, P. Subedi, K. Gao, H. Zhou, P.-L. Lu, P. J. Czoschke, S. Hernandez, M. Ma, R. Lopusnik, Y. Peng, *et al.*, Areal-density limits for heat-assisted magnetic recording and perpendicular magnetic recording, IEEE Transactions on Magnetics **52**, 1 (2016).
- [7] S. D. Granz, T. Ngo, T. Rausch, R. Brockie, R. Wood, G. Bertero, and E. C. Gage, Definition of an areal density metric for magnetic recording Systems, IEEE Transactions on Magnetics **53**, 1 (2017).
- [8] C. Rea, P. Czoschke, P. Krivosik, V. Sapozhnikov, S. Granz, J. Zhu, Y. Peng, J.-U. Thiele, G. Ju, and M. Seigler, High track pitch density for HAMR recording: 1M tpi, IEEE Transactions on Magnetics **55**, 1 (2019).
- [9] D. Suess, T. Schrefl, R. Dittrich, M. Kirschner, F. Dorfbauer, G. Hrkac, and J. Fidler, Exchange spring recording media for areal densities up to 10 Tbit/in², Journal of Magnetism and Magnetic Materials **290-291 PA**, 551 (2005).
- [10] R. H. Victora and X. Shen, Composite media for perpendicular magnetic recording, IEEE Transactions on Magnetics **41**, 537 (2005).
- [11] D. Suess, J. Lee, J. Fidler, and T. Schrefl, Exchange-coupled perpendicular media, Journal of Magnetism and Magnetic Materials **321**, 545 (2009).
- [12] R. F. L. Evans, Q. Coopman, S. Devos, W. J. Fan, O. Hovorka, and R. W. Chantrell, Atomistic calculation of the thickness and temperature dependence of exchange coupling through a dilute magnetic oxide, Journal of Physics D: Applied Physics **47**, 502001 (2014).
- [13] D. Suess, C. Vogler, C. Abert, F. Bruckner, R. Windl, L. Breth, and J. Fidler, Fundamental limits in heat-assisted magnetic recording and methods to overcome it with exchange spring structures, Journal of Applied Physics **117**, 163913 (2015).
- [14] J. Wang, H. Sepehri-Amin, Y. Takahashi, S. Okamoto, S. Kasai, J. Kim, T. Schrefl, and K. Hono, Magnetization reversal of FePt based exchange coupled composite media, Acta Materialia **111**, 47 (2016).
- [15] Z. Liu, Y. Jiao, and R. Victora, Composite media for high density heat assisted magnetic recording, Applied Physics Letters **108**, 232402 (2016).
- [16] P. Chureemart, R. F. L. Evans, R. W. Chantrell, P.-W. Huang, K. Wang, G. Ju, and J. Chureemart, Hybrid design for advanced magnetic recording media: Combining exchange-coupled composite media with coupled granular continuous media, Phys. Rev. Applied **8**, 024016 (2017).
- [17] W. Daeng-am, P. Chureemart, R. W. Chantrell, and J. Chureemart, Granular micromagnetic model for perpendicular recording media: quasi-static properties and media characterisation, Journal of Physics D: Applied Physics **52**, 425002 (2019).
- [18] R.-V. Ababei, M. O. A. Ellis, R. F. L. Evans, and R. W. Chantrell, Anomalous damping dependence of the switching time in fe/fept bilayer recording media, Phys. Rev. B **99**, 024427 (2019).
- [19] X. Zhou, H. Wadley, R. Johnson, D. Larson, N. Tabat, A. Cerezo, A. Petford-Long, G. Smith, P. Clifton, R. Martens, and T. Kelly, Atomic scale structure of sputtered metal multilayers, Acta Materialia **49**, 4005 (2001).
- [20] Computer code VAMPIRE.
- [21] R. F. L. Evans, W. J. Fan, P. Chureemart, M. O. A. Ellis, T. A. Ostler, and R. W. Chantrell, J. Phys.: Condens. Matter **26**, 103202 (2014).
- [22] D. Goll, A. Breitling, and S. Macke, Magnetic Properties of Exchange-Coupled L1₀-FePt/Fe Composite Elements, IEEE Transactions on Magnetics **44**, 3472 (2008).

- [23] F. Casoli, L. Nasi, F. Albertini, S. Fabbri, C. Bocchi, F. Germini, P. Luches, A. Rota, and S. Valeri, Morphology evolution and magnetic properties improvement in FePt epitaxial films by in situ annealing after growth, *Journal of Applied Physics* **103**, 043912 (2008).
- [24] F. Casoli, F. Albertini, L. Nasi, S. Fabbri, R. Cabassi, F. Bolzoni, and C. Bocchi, Strong coercivity reduction in perpendicular fept/fe bilayers due to hard/soft coupling, *Applied Physics Letters* **92**, 142506 (2008).
- [25] D. Goll and A. Breitling, Coercivity of ledge-type L10-FePt/Fe nanocomposites with perpendicular magnetization, *Applied Physics Letters* **94**, 052502 (2009).
- [26] F. Casoli, F. Albertini, L. Nasi, S. Fabbri, R. Cabassi, F. Bolzoni, C. Bocchi, and P. Luches, Role of interface morphology in the exchange-spring behavior of FePt/Fe perpendicular bilayers, *Acta Materialia* **58**, 3594 (2010).
- [27] F. Casoli and G. Varvaro, *Ultra-High-Density Magnetic Recording*, edited by G. Varvaro and F. Casoli (Jenny Stanford Publishing, 2016) p. 528.
- [28] O. N. Mryasov, U. Nowak, K. Y. Guslienko, and R. W. Chantrell, Temperature-dependent magnetic properties of FePt: Effective spin Hamiltonian model, *Europhysics Letters (EPL)* **69**, 805 (2005), 0411020.
- [29] M. O. Ellis and R. W. Chantrell, Switching times of nanoscale FePt: Finite size effects on the linear reversal mechanism, *Applied Physics Letters* **106**, 1 (2015).
- [30] R. V. Ababei, *Atomistic Spin Simulations of Heat Assisted Magnetic Recording Media*, Ph.D. thesis (2019).
- [31] M. Strungaru, S. Ruta, R. F. Evans, and R. W. Chantrell, Model of Magnetic Damping and Anisotropy at Elevated Temperatures: Application to Granular FePt Films, *Physical Review Applied* **14**, 014077 (2020).
- [32] J. U. Thiele, K. R. Coffey, M. F. Toney, J. A. Hedstrom, and A. J. Kellock, Temperature dependent magnetic properties of highly chemically ordered Fe_{55-x}NixPt₄₅ L10 films, *Journal of Applied Physics* **91**, 6595 (2002).
- [33] T. Bublath and D. Goll, Temperature dependence of the magnetic properties of L10-FePt nanostructures and films, *Journal of Applied Physics* **108**, 113910 (2010).
- [34] A. Chernyshov, D. Treves, T. Le, C. Papusoi, H. Yuan, A. Ajan, and R. Acharya, Measurement of magnetic properties relevant to heat-assisted-magnetic-recording, *IEEE Transactions on Magnetics* **49**, 3572 (2013).
- [35] Meo, A and Pantasri, W and Daeng-am, W. and Rannala, S E and Ruta, S I and Chantrell, R W and Chureemart, P. and Chureemart, J, Magnetization dynamics of granular heat-assisted magnetic recording media by means of a multiscale model, *Physical Review B* **102**, 174419 (2020).
- [36] J. Becker, O. Mosendz, D. Weller, A. Kirilyuk, J. C. Maan, P. C. M. Christianen, T. Rasing, and A. Kimel, Laser induced spin precession in highly anisotropic granular L1 0 FePt, *Applied Physics Letters* **104**, 152412 (2014).
- [37] M. O. A. Ellis, M. Galante, and S. Sanvito, Role of longitudinal fluctuations in L10 FePt, *Physical Review B* **100**, 214434 (2019).
- [38] D. A. Garanin, Self-consistent gaussian approximation for classical spin systems: Thermodynamics, *Phys. Rev. B* **53**, 11593 (1996).
- [39] A. di Bona, P. Luches, F. Albertini, F. Casoli, P. Lupo, L. Nasi, S. D'Addato, G. Gazzadi, and S. Valeri, Anisotropy-graded magnetic media obtained by ion irradiation of L10 FePt, *Acta Materialia* **61**, 4840 (2013).
- [40] O. Muthsam, C. Vogler, and D. Suess, Curie temperature modulated structure to improve the performance in heat-assisted magnetic recording, *Journal of Magnetism and Magnetic Materials* **474**, 442 (2018).